Обзор ArXiv: astro-ph, 5-10 декабря 2019

От Сильченко О.К.

ArXiv: 1912.01619

X-shooter Spectroscopy and *HST* Imaging of 15 Ultra Massive Quiescent Galaxies at $z \gtrsim 2$

Mikkel Stockmann,[1,2,3] Sune Toft,[1,2] Anna Gallazzi,[4] Stefano Zibetti,[4] Christopher J. Conselice,[5,6] Berta Margalef-Bentabol,[7] Johannes Zabl,[8] Inger Jørgensen,[9] Georgios E. Magdis,[1,2,10] Carlos Gómez-Guijarro,[1,2,3] Francesco M. Valentino,[1,2,3] Gabriel B. Brammer,[1,2] Daniel Ceverino,[1,2] Isabella Cortzen,[1,2,3] Iary Davidzon,[1,2,11] Richardo Demarco,[12] Andreas Faisst,[11] Michaela Hirschmann,[3] Jens-Kristian Krogager,[13] Claudia D. Lagos,[1,14,15] Allison W. S. Man,[16] Carl J. Mundy,[6] Yingjie Peng,[17] Jonatan Selsing,[1,2,3] Charles L. Steinhardt,[1,2,3] and Kathrine E. Whitaker[18,19]

[1] *Cosmic Dawn Center (DAWN)*

[2] *Niels Bohr Institute, University of Copenhagen, Lyngbyvej 2, 2100 Copenhagen , Denmark*

[3] *DARK, Niels Bohr Institute, University of Copenhagen, Lyngbyvej 2, DK-2100 Copenhagen, Denmark*

Выборка

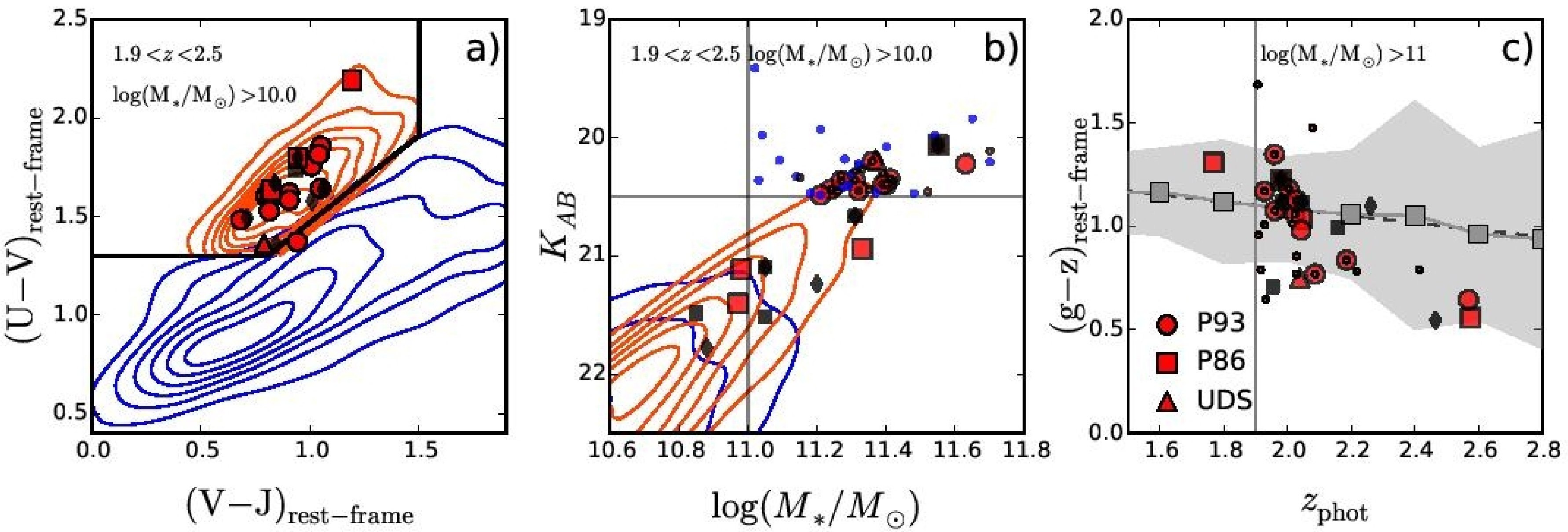

Figure 1. Photometric properties of the galaxy sample (red symbols - see legend on right) in the UVJ (a), the K_{AB}-$\log(M_*/M_\odot)$ (b), and z_{phot}- rest-frame $(g-z)$ planes from the Muzzin et al. (2013a) catalog. Note that for UDS19627 we use the Toft et al. (2012) K-band, stellar mass, z_{phot} and rest-frame colors estimated from the observed photometry with EAZY (Brammer et al. 2011). The UVJ quiescent (red) and star-forming (blue) galaxies are shown in contours in the range $1.9 < z_{phot} < 2.5$ and $\log(M_*/M_\odot) > 10$ (Muzzin et al. 2013a). The spectroscopically confirmed $z > 2$ MQGs from COSMOS are shown with black symbols (square: Krogager et al. (2014), diamond: Belli et al. (2017)). The small red/blue points in (b) are the galaxies that satisfy the criteria $K < 20.5$ and $\log(M_*/M_\odot) > 11$. The gray squares in panel (c) represent the running mean of the rest-frame $(g-z)$ color of the massive, $\log_{10}(M_*/M_\odot) > 11$, UVJ-selected quiescent galaxies with the 1σ standard deviation in gray.

Без звездообразования?

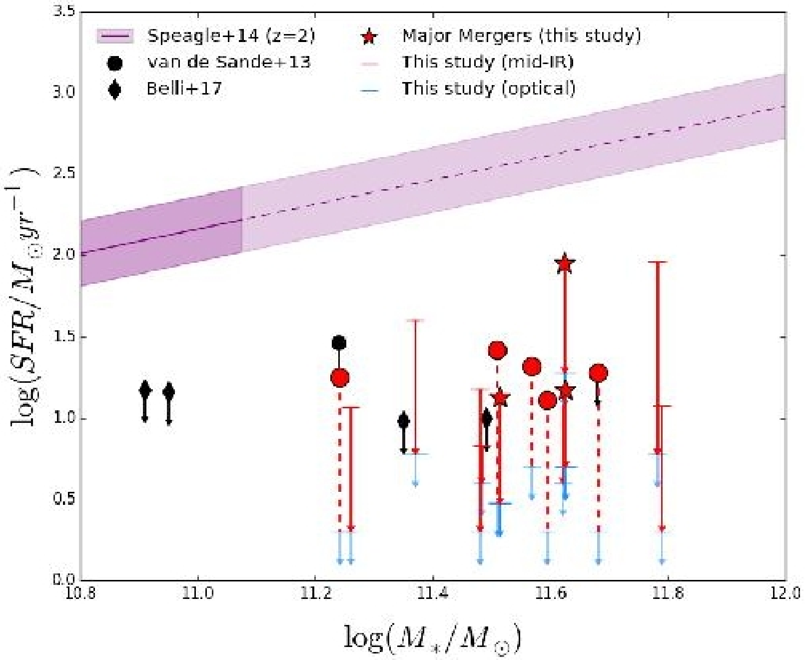

Figure 4. SFR – M_* plane for massive quiescent galaxies at $z > 2$ with 24 μm coverage. The SFR main-sequence at $z = 2$ from Speagle et al. (2014) is shown in dark purple, with its 0.2 dex (1σ) scatter. The light purple region extending beyond $\log(M_*/M_\odot) > 11.1$ is an extrapolation of the best-fit relation. The 24 μm MIPS SFR detections (red circles)/upper limits (red arrows) are shown, with the major mergers (composite measurement of the SFR) in red stars.

Спектры

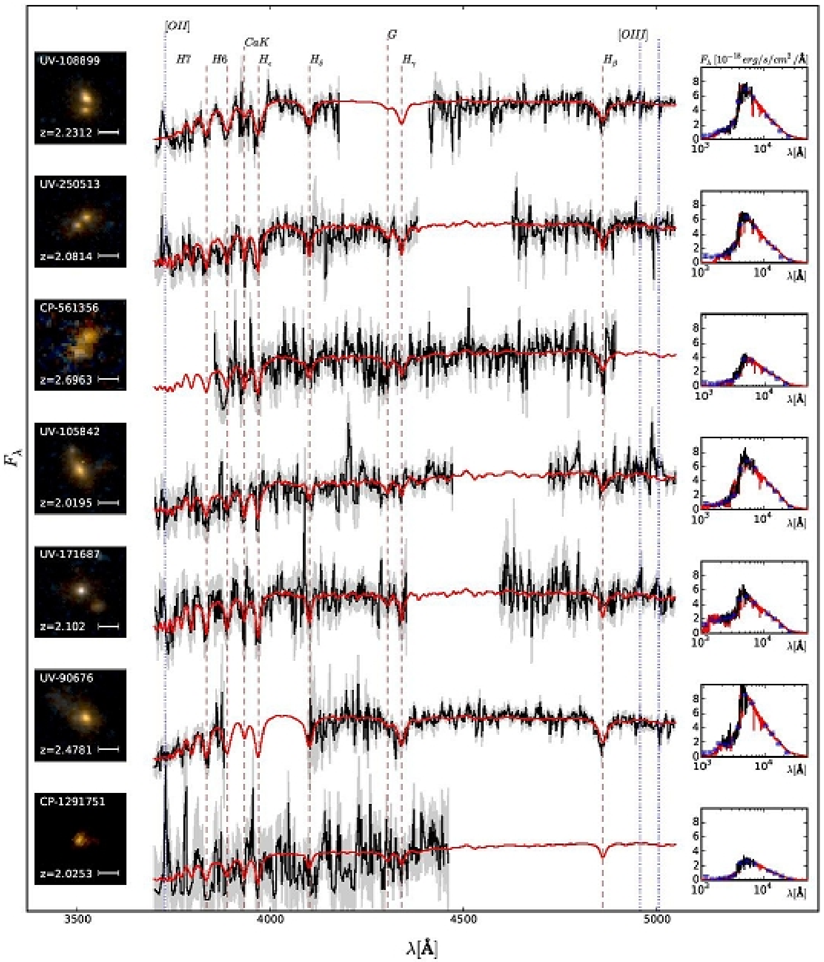
[OII]
H7
H6
CaK
G
[OIII]
UV-108899
z=2.2312
UV-250513
z=2.0814
CP-561356
z=2.6963
UV-105842
z=2.0195
UV-171687
z=2.102
UV-90676
z=2.4781
CP-1291751
z=2.0253
3500
4000
4500
5000
λ[Å]

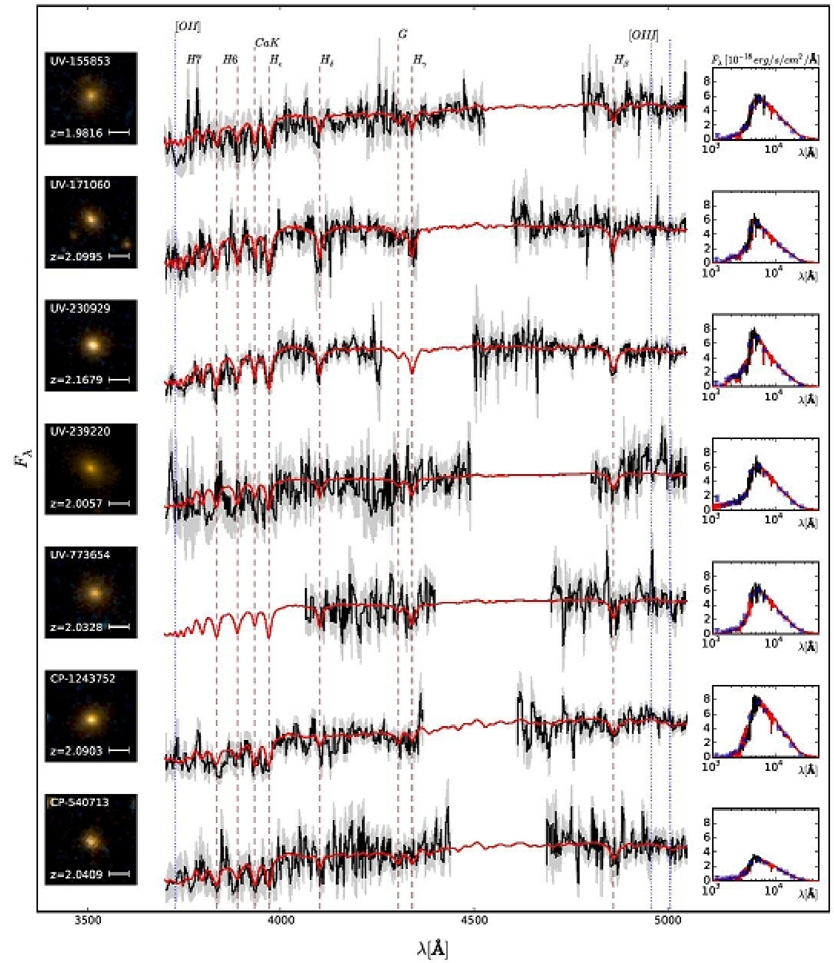
[OII]
H7
H6
CaK
G
[OIII]
UV-155853
z=1.9816
UV-171060
z=2.0995
UV-230929
z=2.1679
UV-239220
z=2.0057
UV-773654
z=2.0328
CP-1243752
z=2.0903
CP-540713
z=2.0409
3500
4000
4500
5000
λ[Å]

Изображения с HST

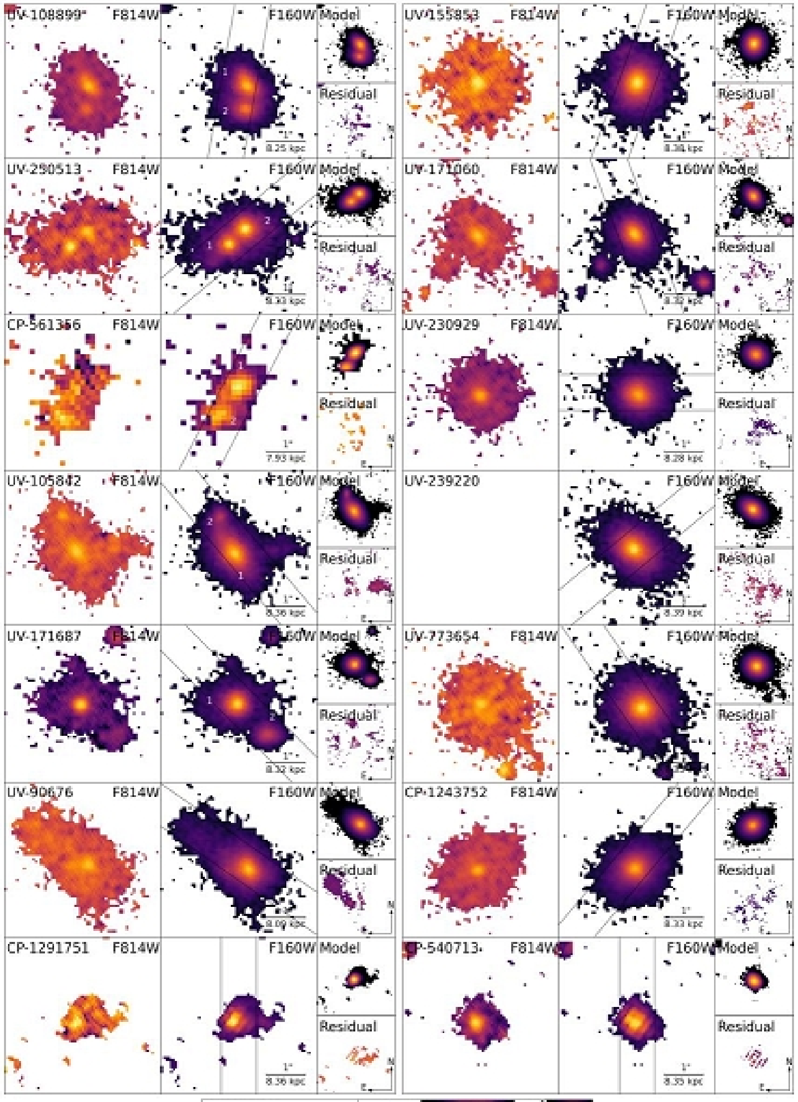

Эволюция дисперсии скоростей и размера: малый мержинг?

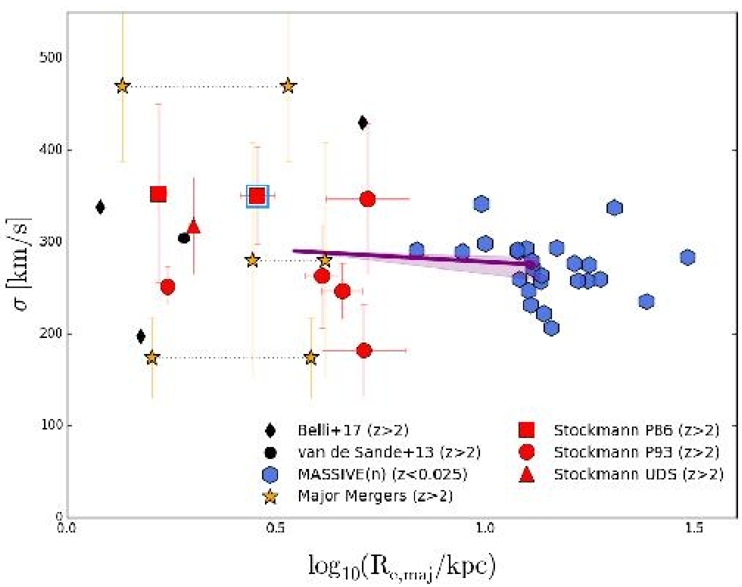

Figure 7. The velocity dispersions are plotted with effective radii for three samples; 1) Our sample (red symbols like Figure 1), 2) massive, $\log_{10}(M_*/M_\odot) > 11$, other quiescent galaxies at $z_{\rm spec} > 2$ (van de Sande et al. 2013; Belli et al. 2017), 3) the MASSIVE(n) sample in blue hexagons. The composite dispersion measurements of the major-merger galaxies are shown in orange stars connecting their individual size measurements with a horizontal dotted line. The blue square indicates our source CP-1243752 (recently published in van de Sande et al. 2013; Kriek et al. 2016; Belli et al. 2017). The purple arrow shows the median evolution between our study and the MASSIVE(n) sample. The uncertainty from the mass rank scatter on the fixed CND is shown in purple shading. The median evolution between the

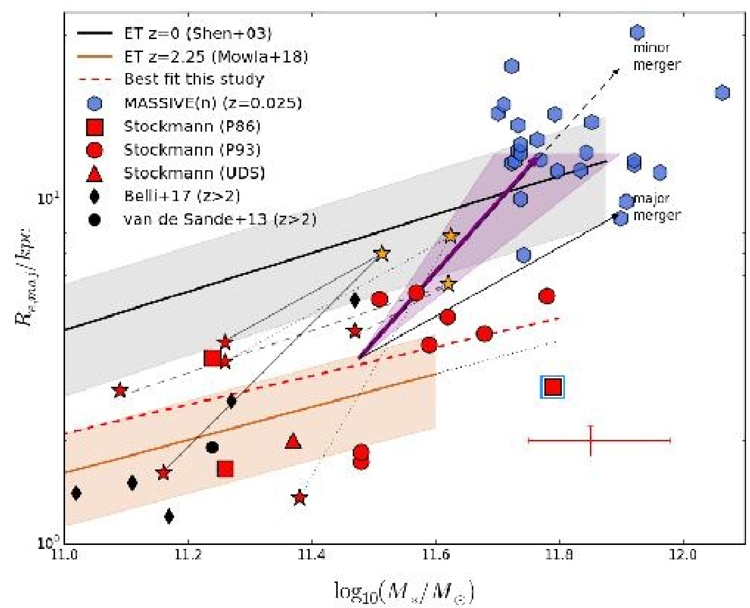

Figure 8. The stellar mass-size plane for massive, $\log_{10}(M_*/M_\odot) > 11.0$, quiescent galaxies: our sample (red symbols), other massive quiescent galaxies at $z > 2$ (black symbols, van de Sande et al. 2013; Belli et al. 2017) and the MASSIVE(n) sample (blue hexagons). The representative error bar of our sample is shown in red. The source CP-1243752 is indicated with a blue square. The ongoing major merger-corrected stellar masses (red stars) are connected (gray dotted, dashed, and solid lines) to their post-merger positions (orange stars), following the Bezanson et al. (2009) prescription. The minor (dashed) and major (solid) merger-predicted evolutions from Bezanson et al. (2009) are shown with black arrows. The best fit relations at $z = 0$ (Shen et al. 2003) and 2.25 (Mowla et al. 2018), with their

Что там со скрытой массой?

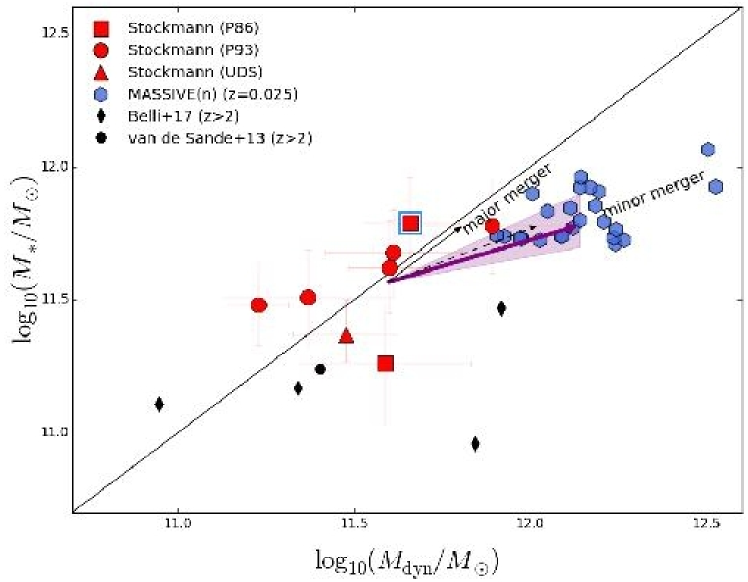

Figure 9. The dynamical-stellar mass plane for this study (red squares: *P86*, circles: *P93*, triangle: UDS19627), other $z_{\rm spec} > 2$ massive quiescent galaxies (in black symbols van de Sande et al. 2013; Belli et al. 2017), and the MASSIVE(n) sample (blue hexagons). The purple arrow connects the median of our sample with the median of the MASSIVE(n) sample. The purple shaded area represents the uncertainty on the median values of the MASSIVE(n) sample from the CND mass rank scatter (see explanation in Section 5.2). The solid black line is the $M_* = M_{\rm dyn}$ relation. The dashed/solid black arrow represents the predicted constant dispersion stellar-to-dynamical mass evolution for minor/major mergers (Bezanson et al. 2009). The blue square indicates the source CP-1243752 (previously published in van de Sande

Выводы: малый мержинг и раздувание звездного тела БЕЗ раздувания гало?

- We find indirect evidence pointing to our velocity dispersion measurements to be minimally contaminated by rotation. Our systems also have a Sérsic index $n > 2.5$ (see Section 5.2). A direct comparison between our study and the MASSIVE(n) sample, shows evidence for shallow or no velocity dispersion evolution from $z = 2 - 0$.

- Our sample is compact, in line with previous studies at $z \sim 2$ (van der Wel et al. 2014; Mowla et al. 2018). We find that the median mass-size evolution ($\Delta r \propto \Delta M_*^\alpha$) compared to the MASSIVE(n) sample is best described by $\alpha = 1.78^{+0.37}_{-0.29}$. This is consistent with both the simple kinematic predictions of minor merger driven size evolution from Bezanson et al. (2009) and the more extensive numerical treatment from Hilz et al. (2012).

- We find that our sample of $z > 2$ MQGs is consistent with a dynamical-to-stellar mass ratio $M_*/M_{\rm dyn} < 1$ but that the shallow dispersion and significant size increase lead to an increasing dynamical-to-stellar mass ratio, doubling from $z = 2$ to the present day. Such an effect is shown to be reproduced for an increasing dark matter fraction from $z = 2 - 0$, within the effective radius of the galaxy (Hilz et al. 2012).

In this paper the largest sample of MQGs at $z > 2$

ArXiv: 1912.03986

Updated fundamental constant constraints from Planck 2018 data and possible relations to the Hubble tension

Luke Hart[1]★ and Jens Chluba[1]
[1]*Jodrell Bank Centre for Astrophysics, Alan Turing Building, University of Manchester, Manchester M13 9PL*

Accepted –. Received –.

ABSTRACT
We present updated constraints on the variation of the fine structure constant, $\alpha_{\rm EM}$, and effective electron rest mass, $m_{\rm e}$, during the cosmological recombination era. These two fundamental constants directly affect the ionization history at redshift $z \simeq 1100$ and thus modify the temperature and polarisation anisotropies of the cosmic microwave background (CMB) measured precisely with *Planck* . The constraints on $\alpha_{\rm EM}$ tighten slightly due to improved *Planck* 2018 polarisation data but otherwise remain similar to previous CMB analysis. However, a comparison with the 2015 constraints reveals a mildly discordant behaviour for $m_{\rm e}$, which from CMB data alone is found below its local value. Adding baryon acoustic oscillation data brings $m_{\rm e}$ back to the fiducial value, $m_{\rm e} = (1.0078 \pm 0.0067)\, m_{\rm e,0}$, and also drives the Hubble parameter to $H_0 = 69.1 \pm 1.2$ [in units of $\rm km\,s^{-1}\,Mpc^{-1}$]. Further adding supernova data yields $m_{\rm e} = (1.0190 \pm 0.0055)\, m_{\rm e,0}$ with $H_0 = 71.24 \pm 0.96$. We perform several comparative analyses using the latest cosmological recombination calculations to further understand the various effects. Our results indicate that a single-parameter extension allowing for a slightly increased value of $m_{\rm e}$ ($\simeq 3.5\sigma$ above $m_{\rm e,0}$) could play a role in the Hubble tension.

Key words: recombination – fundamental physics – cosmology – CMB anisotropies

Почему-то команда Планка не варьирует мировые константы??

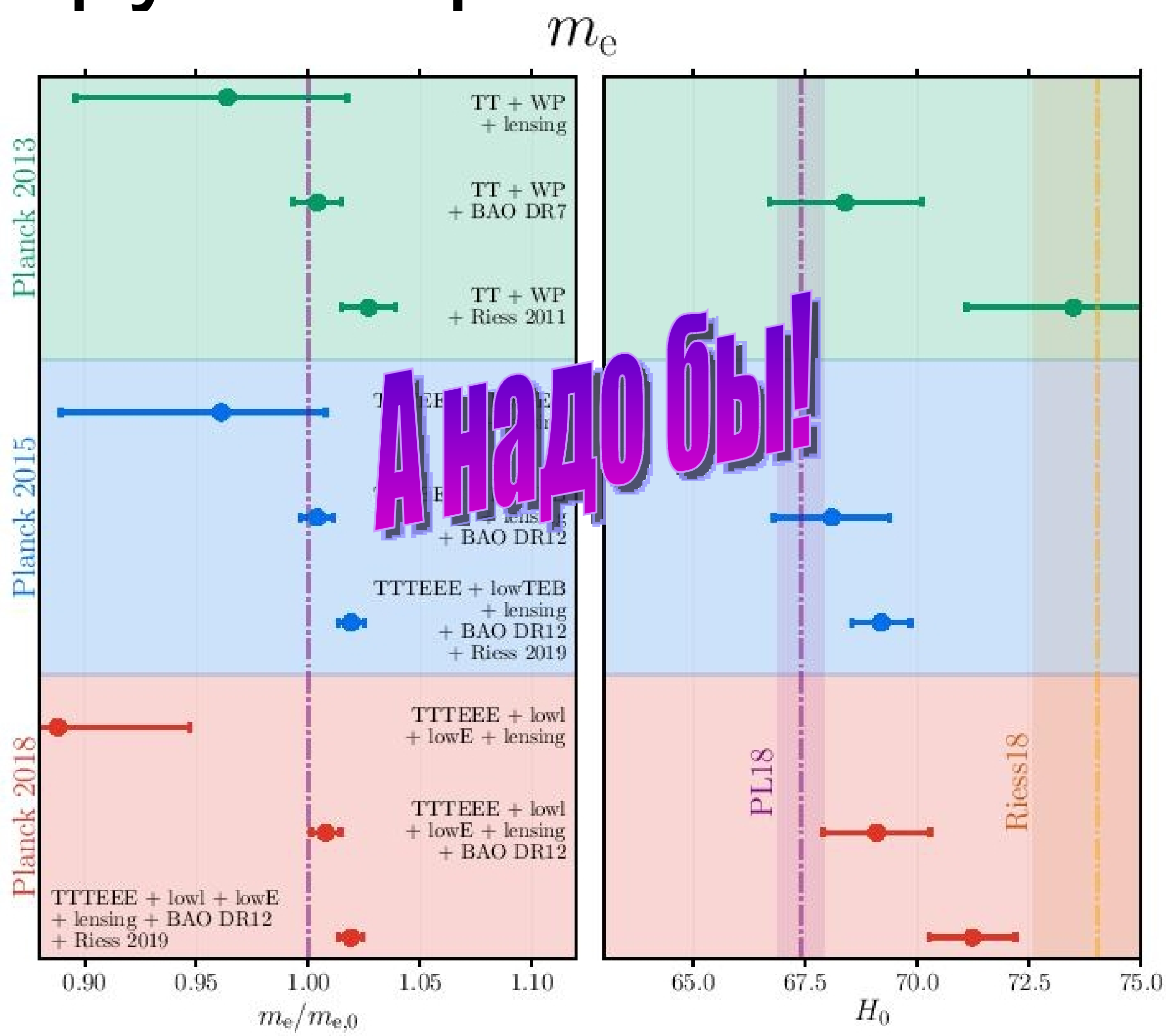

Будут другие результаты для космологических параметров, и получше хи-квадрат

Parameter	*Planck* 2018	*Planck* 2018 + varying $\alpha_{\rm EM}$	*Planck* 2018 + BAO + varying $\alpha_{\rm EM}$	*Planck* 2018 + varying $m_{\rm e}$	*Planck* 2018 + BAO + varying $m_{\rm e}$
$\Omega_b h^2$	0.02237 ± 0.00015	0.02236 ± 0.00015	0.02240 ± 0.00014	$0.0199^{+0.0012}_{-0.0014}$	0.02255 ± 0.00016
$\Omega_c h^2$	0.1199 ± 0.0012	0.1201 ± 0.0014	0.1199 ± 0.0015	0.1058 ± 0.0076	0.1208 ± 0.0018
$100\theta_{MC}$	1.04088 ± 0.00031	1.0416 ± 0.0034	1.0436 ± 0.0030	0.958 ± 0.045	1.0464 ± 0.0047
τ	0.0542 ± 0.0074	0.0540 ± 0.0075	0.0553 ± 0.0075	0.0512 ± 0.0077	0.0549 ± 0.0074
$\ln(10^{10} A_{\rm s})$	3.044 ± 0.014	3.043 ± 0.015	3.043 ± 0.015	3.029 ± 0.017	3.045 ± 0.014
$n_{\rm s}$	0.9649 ± 0.0041	0.9637 ± 0.0070	0.9621 ± 0.0070	0.9640 ± 0.0040	0.9654 ± 0.0040
$\alpha_{\rm EM}/\alpha_{\rm EM,0}$	--	1.0005 ± 0.0024	1.0019 ± 0.0022	--	--
$m_{\rm e}/m_{\rm e,0}$	--	--	--	0.888 ± 0.059	1.0078 ± 0.0067
H_0	67.36 ± 0.54	67.56 ± 0.99	68.32 ± 0.71	46^{+9}_{-10}	69.1 ± 1.2

Table 1. Marginalised values of the fine structure constant and effective electron mass $\alpha_{\rm EM}$ and $m_{\rm e}$ using the *Planck* 2018 data along with BAO contributions. We used a wide prior for H_0 so that the 1σ limit is not cut off and therefore avoids biasing the marginalised $m_{\rm e}$ posterior ($H_0 > 20$).

В частности, можно поправить постоянную Хаббла, если раньше электрон был массивнее

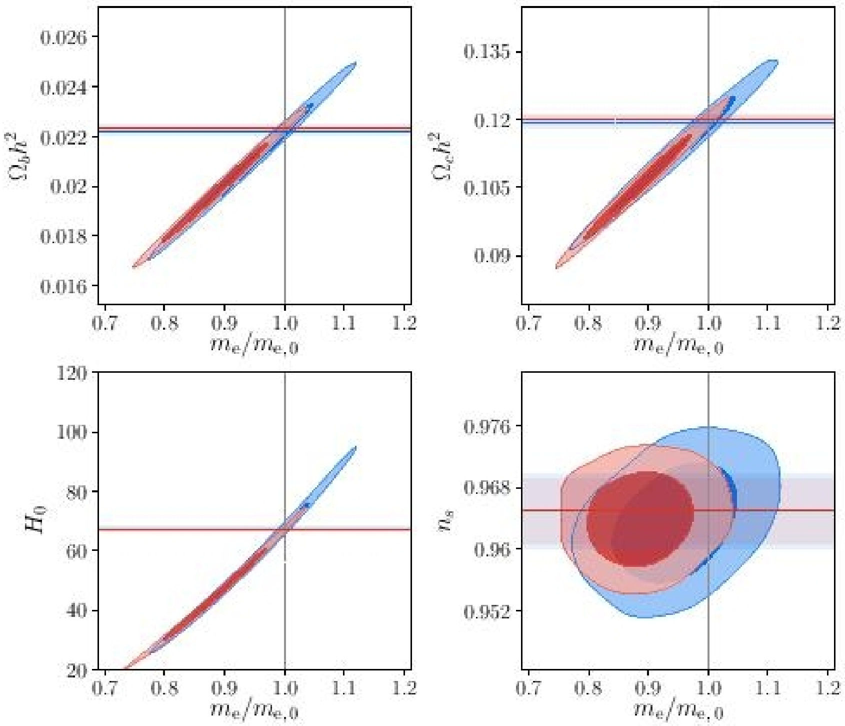

Figure 3. Same as Fig. 2 except here we show the contours for m_e. The same ΛCDM reference marker and fiducial cosmology 1σ bands have been added here. In these contours we ensured $20 < H_0 < 100$.